Differential Sampling Measurement of a 7 V RMS Sine Wave With a Programmable Josephson Voltage Standard

Alain Rüfenacht, Charles J. Burroughs, Jr., Paul D. Dresselhaus, and Samuel P. Benz, *Fellow, IEEE*

***Abstract*—A 10 V programmable Josephson voltage standard has enabled sine waves with voltages up to 7 V RMS to be accurately measured with a differential sampling measurement technique. Expanding the voltage range for this technique enables the direct calibration of the low-frequency ranges of commercial calibrators in the ac voltage mode. This paper reviews the practically achievable performance and challenges of the differential sampling measurement technique that arise when measuring RMS voltages greater than a few volts. A relative Type A uncertainty of 4 parts in 10^7 was achieved with the technique when measuring a 7 V RMS sine wave generated by a calibrator at 62.5 Hz.**[1]

***Index Terms*—Analog-digital conversion, Josephson arrays, power measurement, quantization, signal synthesis, standards, superconductor–normal–superconductor devices, voltage measurement.**

I. Introduction

The National Institute of Standards and Technology (NIST) recently developed a 10 V programmable Josephson voltage standard (PJVS) [1], [2] that allows ac voltage measurements to be extended up to 7 V RMS. Previously, we demonstrated how to implement a differential sampling method with a 2.5 V PJVS for measuring 1.2 V RMS amplitudes for a new electrical power standard at NIST [3]. This straightforward sampling method can characterize any signal up to the maximum voltage of the PJVS by the use of a stepwise-approximated sine wave that is synthesized with the PJVS [4]–[9]. The first demonstrations of the sampling method were accomplished by comparing two PJVS waveforms [4], [5]. Each step of the PJVS waveform provides a quantum-accurate voltage reference at each sample point. The residual differential voltage is measured with a sampling voltmeter in a null-detector configuration. This differential sampling measurement technique is particularly suited for waveform frequencies below 400 Hz. The limitations inherently due to the transients that occur when switching between the quantized voltage steps of the PJVS waveforms [10], [11] are eliminated. Increasing the PJVS voltage to 10 V enables the direct calibration of instruments such as calibrators and digital voltmeters (DVMs) for ac measurements, which currently are calibrated with ac/dc difference measurements by the use of thermal voltage converters.

This paper investigates the performance of the differential sampling technique with the NIST 10 V PJVS, an Agilent 3458A sampling DVM, and a Fluke 5720A calibrator at voltage amplitudes up to 7 V RMS.[2] Comprehensive experimental results are presented that characterize the performance of the instruments, including a calibration curve of the calibrator from 0.5 V to 7 V. Finally, the application of differential sampling by the use of dual PJVS references is presented.

II. Differential Sampling

The differential sampling method combines three main components: a sine-wave voltage source of high spectral purity and stability, a PJVS system to provide the reference voltage waveform, and a sampling DVM to measure differential voltages (see Fig. 1). Other measurement methods that directly apply synthesized waveforms from the PJVS [12]–[14] are limited to applications with high-impedance loads, and the stepwise-approximated waveforms contain harmonics that significantly contribute to the total RMS voltage [15]. The advantage of the differential sampling method is that the output of the sine-wave source can be used directly to drive low-impedance loads [16]. The accuracy of the differential sampling method is limited by the stability of the sine-wave voltage source and the performance of the sampling DVM. All these methods [3]–[9], [12]–[18] implement PJVS systems because they can produce voltages up to 10 V [1], [19]–[21]. Pulse-driven Josephson voltage standards produce intrinsically accurate low-harmonic-content waveforms, but their RMS amplitudes are presently limited to 275 mV [22].

To meet the requirement of spectral purity and stability, we choose a commercial calibrator (Fluke 5720A) as the sine-wave voltage source. The PJVS system is based on the NIST 10 V PJVS array with 265 116 Josephson junctions [1]. The custom bias-current source for the 10 V PJVS system is optimized for both the dc voltage and the stepwise-approximated waveform generation. Since the 10 V PJVS system is not intended to

Manuscript received July 4, 2012; revised October 24, 2012; accepted November 9, 2012. Date of publication February 6, 2013; date of current version May 8, 2013. The Associate Editor coordinating the review process for this paper was Dr. Lucas Di Lillo.

The authors are with the National Institute of Standards and Technology, Boulder, CO 80305-3328 USA (e-mail: alain.rufenacht@nist.gov).

Color versions of one or more of the figures in this paper are available online at http://ieeexplore.ieee.org.

Digital Object Identifier 10.1109/TIM.2013.2237993

[2]Certain commercial equipment, instruments, or materials are identified in this paper to facilitate understanding. Such identification does not imply recommendation or endorsement by NIST, nor does it imply that the materials or equipment that are identified are necessarily the best available for the purpose.

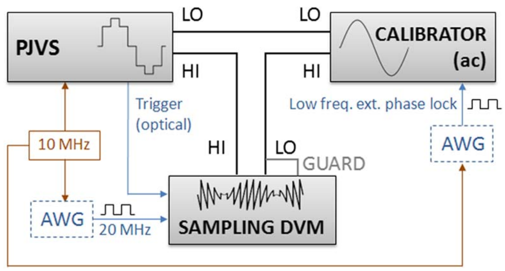

Fig. 1. Block diagram of the differential sampling measurement system.

be used for direct waveform synthesis, due to the limitations induced by the transients [10], [11], a relatively slow current-source rise time ($\tau \cong 2\ \mu$s) is chosen to minimize the ringing of the stepwise-approximated waveform. Pi filters with 0.8 MHz cutoff frequency are used on the current bias, leading to the reduction of the current noise imposed on the PJVS subarrays. Current noise has the effect of reducing the operating margins. Details of the development and implementation of the PJVS are described elsewhere [1], [2], [23]–[25]. The input of the sampling DVM (Agilent 3458A) is connected to the high of both waveforms (see Fig. 1). This configuration simplifies the implementation of the differential sampling in the electrical power standard measurement setup, where two voltage sine waves are compared to the PJVS reference waveform and where the grounding scheme is complex [3]. However, the accuracy of the differential sampling measurements, with this configuration, relies on the common-mode rejection ratio (CMRR) capabilities of the sampling DVM. The error induced by the CMRR of the Agilent 3458A is about 1 part in 10^7 (140 dB) [8]. The guard of the DVM is driven by the calibrator sine wave in order to reduce the influence of capacitive effects.

As shown in the block diagram (see Fig. 1), all three components are time synchronized with the same 10 MHz reference time base. The sampling DVM was modified in order to be locked to an external 20 MHz reference. An optically isolated trigger signal is generated at the start of the PJVS waveform and is provided to the trigger input of the sampling DVM. The DVM sampling windows can be shifted with respect to the trigger signal by an adjustable hardware time delay. This *sampling delay* aligns the sampling windows relative to the PJVS voltage steps in order to avoid contributions from the PJVS transients. The time alignment is optimized for every new PJVS waveform by the use of an automated procedure.

The amplitude of the PJVS waveform is adjusted to match the amplitude of the sine wave. In order to use the sampling DVM in a null-detector configuration, the phase of the calibrator must be adjusted relative to the PJVS waveform to minimize the differential voltage. The calibrator signal frequency is synchronized to that of the PJVS through an intermediary arbitrary waveform generator (AWG) that uses the 10 MHz reference signal as its clock. The AWG produces a square wave at the signal frequency of both the PJVS and calibrator. The *relative phase alignment* of the calibrator signal with respect to the PJVS signal is accomplished by adjusting the phase of the AWG signal.

The differential voltage is measured over multiple periods of the calibrator sine wave (typically 50 periods). The calibrator sine wave is reconstructed by adding the calculated PJVS step voltages to the corresponding measured differences. Since the sampling DVM is integrating the voltage during the aperture period T_{DVM}, all the reconstructed amplitudes must be corrected with the transfer function $\sin(\pi \cdot f \cdot T_{\mathrm{DVM}})/(\pi \cdot f \cdot T_{\mathrm{DVM}})$, where f is the frequency of the signal waveform. A three-parameter sine fit algorithm [26] is applied to the reconstructed waveform in order to extract the amplitude and relative phase of the fundamental, the first ten harmonics, and the residual contributions at the power-line frequency (60 Hz) of the calibrator. The uncertainty is not calculated in the fitting procedure. The full measurement sequence is repeated typically 50 times to obtain an averaged value for the fundamental $(V_{\mathrm{CALIBRATOR}})$. The Type A uncertainty Unc.$(V_{\mathrm{CALIBRATOR}})$ reported is the standard deviation of the mean of $V_{\mathrm{CALIBRATOR}}$. The quantities reported graphically (see Figs. 3–11) are $V_{\mathrm{CALIBRATOR}}$ and Unc.$(V_{\mathrm{CALIBRATOR}})$ with $k = 2$. The contribution of the harmonics and dc offset to the total RMS voltage of the calibrator is negligible compared to the measured Type A uncertainty of the fundamental.

III. Sampling and Measurement Constraints

The waveform generated by the PJVS system is a stepwise-approximated sine wave, where the voltage on the jth step is given by $V_P \cdot \sin(2\pi j/N) + \delta_j$, where N is the number of PJVS steps per period, V_P is the nominal peak amplitude of the calibrator, and δ_j is the correction due to the quantization of the PJVS voltage. δ_j is smaller than the voltage given by the least significant bit of the NIST 10 V array (230 μV, which is equivalent to the voltage step produced by six Josephson junctions with an applied microwave frequency of 18.275 GHz). The sampling voltmeter integrates the voltage difference between the PJVS waveform and the calibrator sine wave for every PJVS step over a time interval T_{DVM} (see Fig. 2). The aperture ratio is defined as $r = T_{\mathrm{DVM}}/T_{\mathrm{STEP}}$, and the duration of each PJVS step is $T_{\mathrm{STEP}} = (N \cdot f)^{-1}$. The value of r is chosen to fulfill the condition $T_{\mathrm{STEP}} - T_{\mathrm{DVM}} \geq 30\ \mu$s so that the sampling DVM has enough time to complete its required setup time and provide its highest accuracy.

This sampling method is slightly different from the one used in the previous work [6], where two sampling windows were used for each PJVS step and the window aligned with the transients between steps was discarded. In the current work, we achieve 20% longer sampling times $(r = 0.7)$ by using a single sampling window for each PJVS step and adjusting the sampling delay so that the window excludes the transient regions between steps.

The integrated voltage difference for the jth sampling window is given by the expression

$$\Delta V_{\mathrm{DVM}}(j) = V_P \cdot \sin(2\pi j/N) + \delta j - V_C N/(2\pi r) \cdot [\cos(2\pi(j - r/2)/N + \phi) - \cos(2\pi(j + r/2)/N + \phi)]$$

where V_C is the peak voltage of the calibrator and ϕ is the "relative phase difference" of the calibrator sine wave with respect to the PJVS waveform. ΔV_{DVM} is the voltage difference of the integrated value of the calibrator sine wave with respect to the PJVS step voltage (graphically represented as a dot in the center

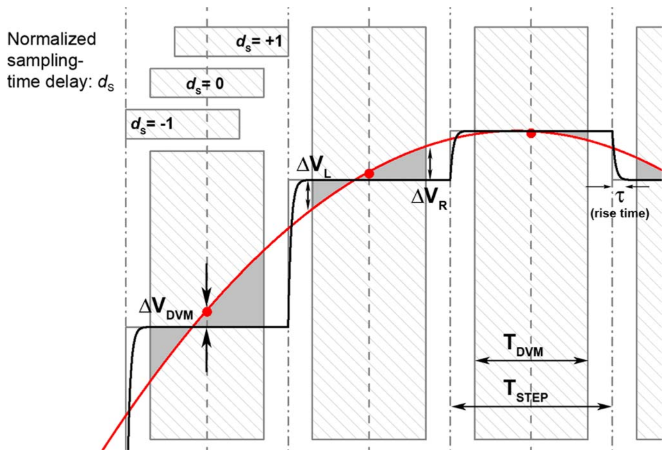

Fig. 2. (Color online) Time-alignment sketch of the three differential sampling components. (Black) PJVS stepwise-approximated sine wave. (Red) Calibrator sine wave. (Gray rectangular boxes) Voltmeter sampling window. For each PJVS voltage step, the sampling voltmeter integrates the (gray area) voltage difference between the PJVS and the calibrator. For each sampling window, the (red dot) measured differential voltage ΔV_{DVM} is displayed relative to the PJVS waveform step voltage.

of the sampling window in Fig. 2). The voltage differences at the beginning (ΔV_L) and at the end (ΔV_R) of each sampling window are

$$\begin{aligned}\Delta V_L(j) &= V_P \cdot \sin(2\pi j/N) + \delta j - V_C \\ &\quad \cdot \sin\left(2\pi(j - r/2)/N + \phi\right), \text{ and} \\ \Delta V_R(j) &= V_P \cdot \sin(2\pi j/N) + \delta j - V_C \\ &\quad \cdot \sin\left(2\pi(j + r/2)/N + \phi\right).\end{aligned}$$

In the ideal case, when the phase is perfectly adjusted ($\phi = 0$) and $V_C = V_P$, the maximal voltage difference $(\Delta V_{\mathrm{MAX}})$ occurs on the $j = 0$ step

$$\Delta V_{\mathrm{MAX}} = \Delta V_R(0) = -\Delta V_L(0) = V_C \cdot \sin(\pi \cdot r/N) \cong V_C \cdot \pi \cdot r/N.$$

The voltage range selected for the sampling DVM must be larger than ΔV_{MAX}. Measurements on the 1 V range of the DVM result in higher measurement noise compared with the 100 mV range. In order to measure the differential voltage on the 100 mV range ($\Delta V_{\mathrm{MAX}} \le 100$ mV) with a calibrator amplitude of 7 V RMS (equivalent to a peak value $V_C = 10$ V), the ratio N/r must be at least 315. In reality, this ratio is larger since a perfect phase alignment is difficult to achieve. Increasing N or decreasing r leads to the same consequence: a reduction of the aperture time of the DVM and a corresponding increase in the measurement noise. The dependence of the DVM noise on the aperture time is described in [5]. Fortunately, if the sine-wave source has good short-term and long-term stabilities, then this effect can be compensated with longer averaging.

IV. Measurements

A. Differential Measurements at 7 V RMS

A complete set of measurements was conducted in order to verify that the measurement method produces results that are sufficiently independent of the measurement parameters. The ability to measure the RMS voltage of the calibrator with

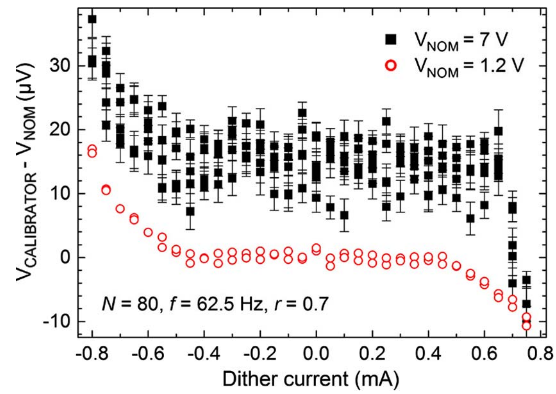

Fig. 3. Dither-current flat-spot measurement for verifying the quantization (or "flat spot" operating margin) of the PJVS waveform. Both amplitudes (7 V and 1.2 V) show flat constant-voltage plateaus over a current range of at least 0.9 mA.

the differential sampling method must be independent over a reasonable range of the following:

1) PJVS settings, such as the dither current [1], [10], [11] and the number of steps per period;
2) the phase of the calibrator sine wave;
3) the sampling delay of the DVM integration window;
4) the amplitude mismatch between the sine wave and PJVS waveform.

For most of the measurements presented in this section, the calibrator was set to a constant RMS amplitude of $V_{\mathrm{NOM}} = 7$ V and a frequency of $f = 62.5$ Hz. The range of the sampling voltmeter was 1 V. With $N = 80$ and $r = 0.7$, the transfer function correction factor is 0.999 874 064.

Before and after every differential measurement sequence, the quantization of the array at 10 V was confirmed by use of the dc dither-current flat-spot procedure [1]. Additionally, the quantization of the PJVS array in ac mode was verified while generating the 7 V RMS stepwise-approximated waveform. Fig. 3 shows the measured calibrator amplitude for $V_{\mathrm{NOM}} = 7$ V and $V_{\mathrm{NOM}} = 1.2$ V as a function of the dither current. The voltage noise of the calibrator at 1.2 V is lower than that at 7 V, allowing a more precise determination of the flat-spot limits. The rounding observed at each end of the plateau indicates the current where the PJVS begins to deviate from quantum behavior. Within the measurement uncertainty, the PJVS produces a constant voltage over a current range of at least 0.9 mA, confirming that all of the junctions in the array are generating quantized behavior to produce the stepwise-approximated waveform. Fig. 4 shows no variation of the calibrator amplitude when the number of PJVS steps per period is varied from 40 to 256. This result confirms that the differential sampling method is independent of N in the range from 40 to 256 and within the measured uncertainty.

Each sampling voltmeter integration window needs to be carefully aligned with respect to its corresponding PJVS waveform step in order to avoid the transients occurring between the steps. Fig. 5 shows the measured calibrator amplitude versus the sampling delay. The sampling delay is achieved by shifting the sampling window by a delay t_S relative to the center of the PJVS step. For clarity, the abscissa of Fig. 5 is defined as

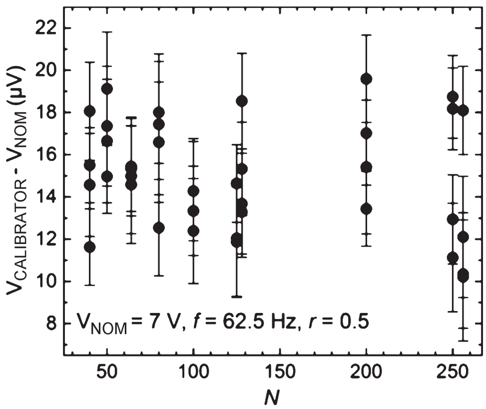

Fig. 4. Measurement of the calibrator amplitude as a function of the number of PJVS waveform steps per period (N) shows that the measurement is independent of step number over the range from 40 to 256.

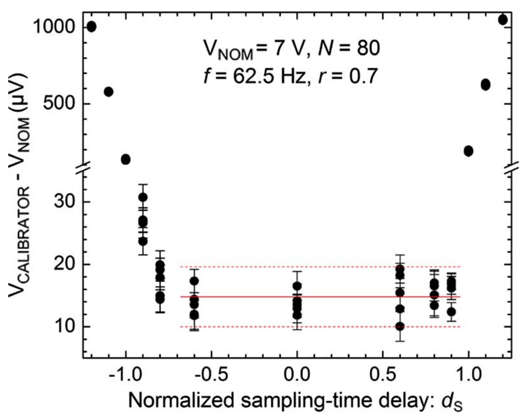

Fig. 5. Measurement of the calibrator RMS amplitude for different sampling-time delays between the sampling voltmeter integration window and the PJVS waveform (see upper left corner of Fig. 2 and text for details). The solid line represents the mean value, and the dashed lines represent the standard deviation $(k = 2)$ of $V_{\mathrm{CALIBRATOR}}$ between $d_S = -0.6$ and $d_S = 0.9$.

a normalized quantity $d_S = 2t_S/(T_{\mathrm{STEP}} - T_{\mathrm{DVM}}) = 2t_S N f \cdot (1 - r)$. $V_{\mathrm{CALIBRATOR}}$ is constant over the delay range from -0.6 to $+0.9$, within the measured uncertainty of 4.8 μV $(k = 2)$. The measured amplitude deviates from the nominal value very gradually near the $d_S = -0.8$ corner due to the finite rise time of the bias electronics $(\tau \cong 2\ \mu\mathrm{s})$.

To take full advantage of the differential sampling method, the sampling voltmeter must be used in a null-detector configuration. The relative phase alignment of the calibrator sine wave must be correctly adjusted in order to minimize the differential voltage. However, the measurement method should still produce the correct amplitude even if the phase of the calibrator is not perfectly aligned. Fig. 6 shows the calibrator amplitude as a function of the relative phase. The measured calibrator amplitudes, over a $\pm 2^\circ$ range of variation of the phase, give the same result as the measurements performed at 0°, where $V_{\mathrm{CALIBRATOR}} - V_{\mathrm{NOM}} = (15.8 \pm 5.7)$ μV, $(k = 2)$. The method was not tested outside of this range.

As described earlier in the sampling and measurement constraints section, it is important to evaluate the performance of the sampling DVM as the differential voltage within the sampling windows is increased. One measurement is to vary the aperture ratio (r) of the DVM while keeping the DVM range unchanged at 1 V. Based on earlier measurements

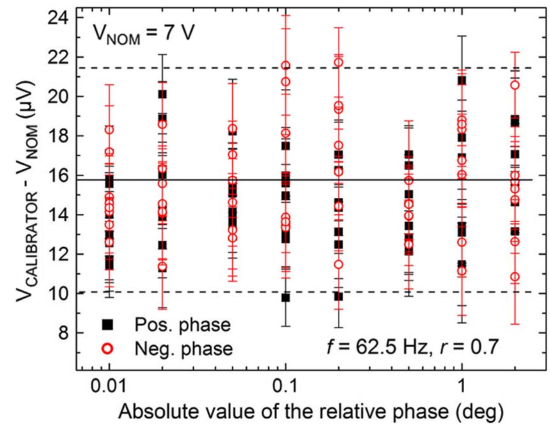

Fig. 6. Dependence of the measured calibrator amplitude versus its phase alignment relative to the PJVS waveform. The averaged calibrator amplitude with a phase alignment at 0° is represented by the horizontal solid line, and the standard deviation $(k = 2)$ is represented by the two dashed lines.

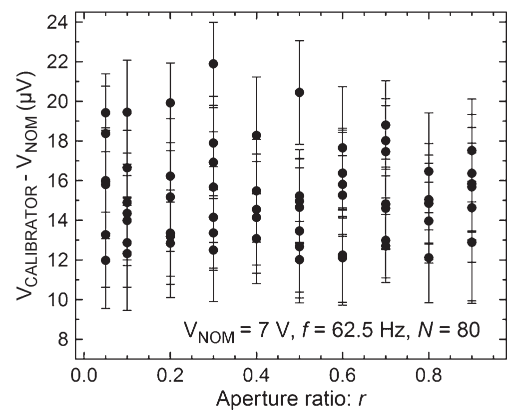

Fig. 7. Measurement of the calibrator RMS amplitude versus the aperture ratio of the voltmeter.

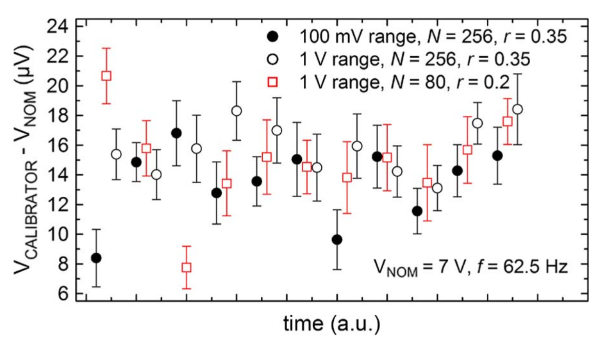

Fig. 8. Measurement of the calibrator RMS amplitude for different DVM ranges demonstrating reproducibility of the measurement technique and independence of DVM range. The measurement duration lasts 3 min for a single measurement point and 5 h for the entire sequence represented.

performed between two PJVS systems [5], reducing the DVM aperture time is expected to increase the uncertainty of the measured calibrator amplitude. However, large aperture times produce large voltages at the beginning and at the end of each integration window (see the quantities ΔV_L and ΔV_R defined earlier). In Fig. 7, no variation of either the amplitude or its associated uncertainty is observed for aperture ratios up to 0.9. Increasing N and reducing r allow the measurement of the differential voltage on the lower 100 mV range of the sampling DVM instead of the 1 V range. Fig. 8 shows a number of

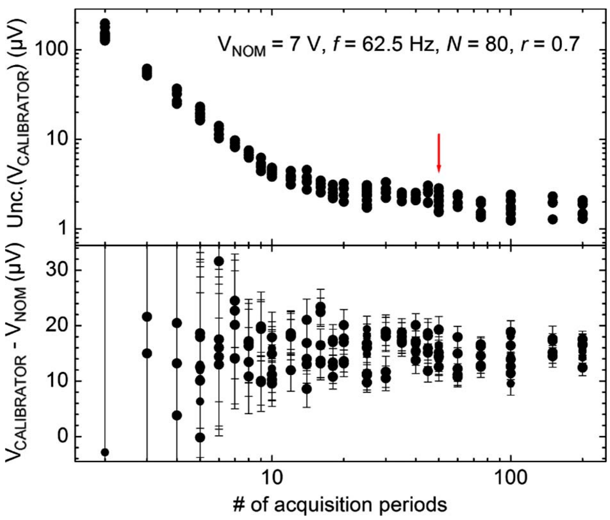

Fig. 9. Dependence of the (top) $k = 2$ Type A uncertainty and (bottom) calibrator RMS measured amplitude versus the number of acquisition periods used for determination of $V_{\mathrm{CALIBRATOR}}$ with the sine fit. The arrow indicates the standard number of acquisition periods used (50) for all the other measurements described in this paper.

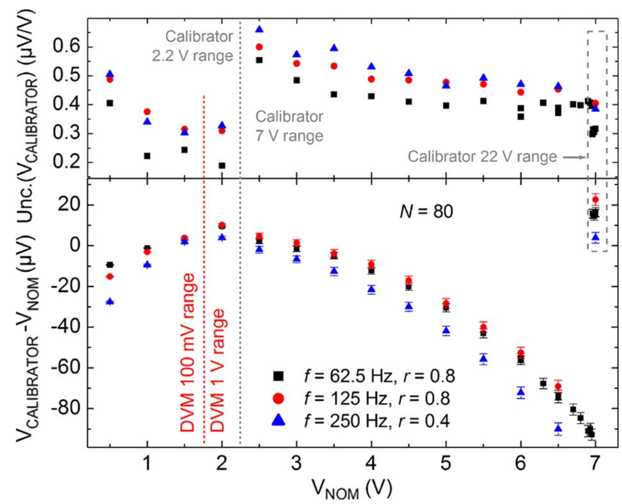

Fig. 10. Dependence of the (bottom) calibrator RMS amplitude on the nominal amplitude for three different frequencies for the three lowest calibrator voltage ranges. (Top) Corresponding relative Type A uncertainty $(k = 2)$.

measured results that were produced with different DVM range and aperture settings and different numbers of PJVS steps. The mean values of the measured calibrator amplitudes $(N=80)$, $V_{\mathrm{CALIBRATOR}} - V_{\mathrm{NOM}} = (13.4 \pm 5.2)$ μV and $V_{\mathrm{CALIBRATOR}} - V_{\mathrm{NOM}} = (15.8 \pm 3.6)$ μV for the 100 mV and the 1 V range, respectively, agree within their measured uncertainties $(k = 2)$. The results of Figs. 7 and 8 strongly suggest that the uncertainty of these measurements is not limited by the sampling voltmeter capabilities, but rather is dominated by the amplitude stability and phase jitter of the calibrator. The effects described in the sampling and measurement constraints section remain, and a source with better performance is required to characterize the measurement limitations.

The amplitude of the calibrator is derived from a sine fitting of the reconstructed waveform. The uncertainty of the measured amplitude depends on the number of periods used for the sine fit. As shown in Fig. 9, at least 50 acquisition periods of the 62.5 Hz calibrator sine wave are necessary to minimize the uncertainty. The measured Type A uncertainty $(k = 2)$ of the calibrator at 7 V and 62.5 Hz is 2.6 μV, corresponding to a relative uncertainty of 4 parts in 10^7.

B. Linearity of the Calibrator

The 10 V amplitude of the NIST PJVS system allows the differential sampling method to directly calibrate the sine-wave amplitude of calibrators, over its first five ranges (100% coverage of the 2.2 mV–2.2 V ranges and 32% coverage of the 22 V range). The differential sampling method measures the gain and linearity of the calibrator ranges automatically, and the measurements can be performed more quickly than conventional methods that use thermal transfer standards. The traceability to the primary standard is similarly as direct as the methods commonly used for calibrating secondary dc standards. Fig. 10 shows the voltage difference between the measured and nominal values of the calibrator from 0.5 V to 7 V generated on three calibrator output ranges (2.2 V, "7 V," and 22 V). Note that the "7 V" range mentioned in this paper cannot be selected directly on the instrument. It appears that the amplitude feedback ac/dc transfer module inside the calibrator uses an internal 7 V range. The voltages vary monotonically from the nominal values differently for each range (around 40 μV for the 2.2 V range and 100 μV for the "7 V" range). These values are still smaller than the uncertainty quoted by the calibrator manufacturer. A discontinuity in the measured calibrator amplitudes occurs at 6.96 V due to the internal range switch. Nearly identical voltage dependences are observed for the three different frequencies that were measured. These frequency and amplitude variations are characteristics of this calibrator. Similar behavior was observed by Jeanneret *et al.*, by the use of a different measurement method [27], suggesting that these results may be typical of the Fluke calibrators. Our differential sampling method can perform direct calibrations up to frequencies of 400 Hz (not shown). At $f = 400$ Hz and with $N = 50$ and $r \leq 0.4$, the criteria $T_{\mathrm{STEP}} - T_{\mathrm{DVM}} = (1 - r) \cdot (N \cdot f)^{-1} \geq 30$ μs are still satisfied. A faster sampling DVM, with similar noise characteristics as that of the Agilent 3458A in the dc sampling mode, will be required in order to measure the calibrator at higher frequencies [5].

C. Dual-Amplitude PJVS Reference Waveform

In the previous work for calibrating electrical power meters [3], we developed a differential sampling method capable of measuring two sine waves of different amplitudes by the use of one PJVS system that synthesized a dual-amplitude reference waveform [3], [6]. Each sine wave has its own dedicated sampling DVM. The dual-amplitude waveform consists of multiple periods of the first reference waveform juxtaposed with the same number of periods of the second reference waveform. The concept of dual waveform can easily be extended to three or more references with different amplitudes and frequencies. The 10 V PJVS current bias source memory is currently limited to 2048 samples, which allows the generation of two juxtaposed

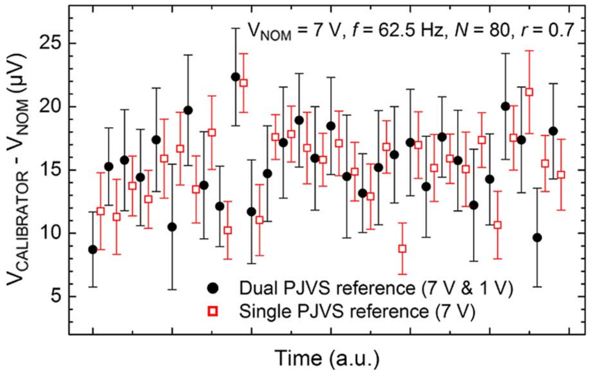

Fig. 11. Measurement of the calibrator RMS voltage with dual and single PJVS references. The measurement duration lasts 2 min for a single measurement point and 7 h for the entire sequence represented.

PJVS reference waveforms with $N = 80$ step/periods repeated over 12 periods each. The first measured period of each waveform is discarded from the fitting procedure in order for the sampling DVM to recover from the overloaded state that occurs while the alternate waveform of mismatched amplitude produces undesirable large differential voltages to the DVM input [6]. Fig. 11 presents the results of alternating measurements of a single PJVS reference at 7 V RMS and a dual PJVS reference with 12 periods of 7 V RMS amplitude followed by 12 periods of 1 V RMS. The RMS amplitude of the calibrator is set to $V_{\mathrm{NOM}} = 7$ V. No difference in the measured amplitude of the calibrator is observed, confirming the validity of the dual PJVS reference method with waveforms of larger amplitude. Note that the measured uncertainty achieved with the dual PJVS reference is slightly larger as a result of the smaller number of acquisition periods (11 periods) used for the fitting algorithm (see Fig. 8).

V. Conclusion

The results obtained confirm the capabilities of using the NIST 10 V PJVS system to measure sine-wave sources with RMS amplitudes up to 7 V with the differential sampling method. Now that higher PJVS voltages are available, differential sampling can be applied to a wider range of voltage metrology applications, such as the direct calibration of commercial calibrators for both dc and ac voltages. The differential sampling method has the advantage of providing direct traceability to a quantum standard. However, two obstacles remain in order to extend the application range of PJVS systems with the differential sampling method. First, in order to be applicable to RMS calibrations, the PJVS must be integrated with a sine-wave voltage source with low harmonic content that has excellent short-term and long-term stabilities. Calibrators provide a good temporary solution for this source, but the phase jitter and the short-term amplitude fluctuation limit their accuracy to the range from 0.2 to 1 part in 10^6. Sources with better amplitude and jitter performance are critical for reducing the measurement uncertainty and implementing the differential sampling method for precision ac measurements [28]. The second obstacle is extending the frequency range of the PJVS differential sampling method above 400 Hz. Implementation of the technique with a high-resolution high-speed analog-to-digital converter will be necessary.

Acknowledgment

The authors would like to thank T. Nelson for providing the Fluke calibrator, B. Waltrip for the helpful discussions regarding the differential sampling method and for providing the external clock reference circuit board implemented in the digital voltmeter, and M. Elsbury and D. Olaya for the contributions in developing the National Institute of Standards and Technology 10 V PJVS array.

References

[1] C. J. Burroughs, P. D. Dresselhaus, A. Rüfenacht, D. Olaya, M. M. Elsbury, Y. Tang, and S. P. Benz, "NIST 10 V programmable Josephson voltage standard system," *IEEE Trans. Instrum. Meas.*, vol. 60, no. 7, pp. 2482–2488, Jul. 2011.

[2] P. D. Dresselhaus, M. M. Elsbury, and S. P. Benz, "Tapered transmission lines with dissipative junctions," *IEEE Trans. Appl. Supercond.*, vol. 19, no. 3, pp. 993–998, Jun. 2009.

[3] B. C. Waltrip, B. Gong, T. L. Nelson, Y. Wang, C. J. Burroughs, A. Rüfenacht, S. P. Benz, and P. D. Dresselhaus, "AC power standard using a programmable Josephson voltage standard," *IEEE Trans. Instrum. Meas.*, vol. 58, no. 4, pp. 1041–1048, Apr. 2009.

[4] R. Behr, L. Palafox, G. Ramm, H. Moser, and J. Melcher, "Direct comparison of Josephson waveforms using an ac quantum voltmeter," *IEEE Trans. Instrum. Meas.*, vol. 56, no. 2, pp. 235–238, Apr. 2007.

[5] A. Rüfenacht, C. J. Burroughs, and S. P. Benz, "Precision sampling measurements using ac programmable Josephson voltage standards," *Rev. Sci. Instrum.*, vol. 79, no. 4, pp. 044704-1–044704-9, Apr. 2008.

[6] A. Rüfenacht, C. J. Burroughs, S. P. Benz, P. D. Dresselhaus, B. C. Waltrip, and T. L. Nelson, "Precision differential sampling measurements of low-frequency voltages synthesized with an programmable Josephson voltage standard," *IEEE Trans. Instrum. Meas.*, vol. 58, no. 4, pp. 809–815, Apr. 2009.

[7] A. Rüfenacht, C. J. Burroughs, P. D. Dresselhaus, and S. P. Benz, "Differential sampling measurement of a 7 V rms sine wave and a programmable Josephson voltage standard," in *Proc. CPEM*, Washington, DC, Jul. 1–6, 2012, pp. 174–175.

[8] M.-S. Kim, K.-T. Kim, W.-S. Kim, Y. Chong, and S.-W. Kwon, "Analog-to-digital conversion for low-frequency waveforms based on the Josephson voltage standard," *Meas. Sci. Technol.*, vol. 21, no. 11, pp. 115102-1–115102-6, Nov. 2010.

[9] J. M. Williams, D. Henderson, J. Pickering, R. Behr, F. Müller, and P. Scheibenreiter, "Quantum-referenced voltage waveform synthesiser," *IET Sci. Meas. Technol.*, vol. 5, no. 5, pp. 163–174, Sep. 2011.

[10] C. J. Burroughs, A. Rüfenacht, S. P. Benz, P. D. Dresselhaus, B. C. Waltrip, and T. L. Nelson, "Error and transient analysis of stepwise approximated sine waves generated by programmable Josephson voltage standards," *IEEE Trans. Instrum. Meas.*, vol. 57, no. 7, pp. 1322–1329, Jul. 2008.

[11] C. J. Burroughs, A. Rüfenacht, S. P. Benz, and P. D. Dresselhaus, "Systematic error analysis of stepwise-approximated ac waveforms generated by a programmable Josephson voltage standard," *IEEE Trans. Instrum. Meas.*, vol. 58, no. 4, pp. 761–767, Apr. 2009.

[12] G. Eklund, T. Bergsten, V. Tarasso, and K.-E. Rydler, "Determination of transition error corrections for low frequency stepwise-approximated Josephson sine waves," *IEEE Trans. Instrum. Meas.*, vol. 60, no. 7, pp. 2399–2403, Jul. 2011.

[13] O. Séron, S. Djordjevic, I. Budovsky, T. Hagen, R. Behr, and L. Palafox, "Precision ac-dc transfer measurements with a Josephson waveform synthesizer and a buffer amplifier," *IEEE Trans. Instrum. Meas.*, vol. 61, no. 1, pp. 198–204, Jan. 2012.

[14] C. J. Burroughs, A. Rüfenacht, S. P. Benz, and P. D. Dresselhaus, "Method for ensuring accurate ac waveforms with programmable Josephson voltage standards," *IEEE Trans. Instrum. Meas.,* IM-12-6239-R1, accepted for publication.

[15] C. J. Burroughs, S. P. Benz, P. D. Dresselhaus, B. C. Waltrip, T. L. Nelson, Y. Chong, J. M. Williams, D. Henderson, P. Patel, L. Palafox, and R. Behr, "Development of a 60 Hz power standard using

SNS programmable Josephson voltage standards," *IEEE Trans. Instrum. Meas.*, vol. 56, no. 2, pp. 289–294, Apr. 2007.

[16] A. Rüfenacht, F. Overney, A. Mortara, and B. Jeanneret, "Thermal transfer standard validation of the Josephson-voltage-standard-locked sine wave synthesizer," *IEEE Trans. Instrum. Meas.*, vol. 60, no. 7, pp. 2372–2377, Jul. 2011.

[17] J. Lee, J. Schurr, J. Nissilä, L. Palafox, and R. Behr, "The Josephson two-terminal-pair impedance bridge," *Metrologia*, vol. 47, no. 4, pp. 453–459, Aug. 2010.

[18] I. Budovsky, D. Geogakopoulos, T. Hagen, H. Sasaki, and H. Yamamori, "Precision ac-dc difference measurement system based on a programmable Josephson voltage standard," *IEEE Trans. Instrum. Meas.*, vol. 60, no. 7, pp. 2439–2444, Jul. 2011.

[19] H. Yamamori, M. Itoh, H. Sasaki, A. Shoji, S. P. Benz, and P. D. Dresselhaus, "10 V programmable Josephson voltage standard circuits using NbN/TiNx/NbN/TiNx/NbN double junction stacks," *Appl. Phys. Lett.*, vol. 88, no. 4, pp. 042503-1–042503-3, Jan. 2006.

[20] F. Müller, R. Behr, L. Palafox, J. Kohlmann, R. Wendisch, and I. Krasnopolin, "Improved 10 V SINIS series arrays for applications in ac voltage metrology," *IEEE Trans. Appl. Supercond.*, vol. 17, no. 2, pp. 649–652, Jun. 2007.

[21] F. Mueller, R. Behr, T. Weimann, L. Palafox, D. Olaya, P. D. Dresselhaus, and S. P. Benz, "1 V and 10 V SNS programmable voltage standards for 70 GHz," *IEEE Trans. Appl. Supercond.*, vol. 19, no. 3, pp. 981–986, Jun. 2009.

[22] S. P. Benz, P. D. Dresselhaus, A. Rüfenacht, N. F. Bergren, J. R. Kinard, R. P. Landim, and T. L. Nelson, "Progress toward a 1 V pulse-driven ac Josephson voltage standard," *IEEE Trans. Instrum. Meas.*, vol. 58, no. 4, pp. 838–843, Apr. 2009.

[23] C. A. Hamilton, C. J. Burroughs, and R. L. Kautz, "Josephson D/A converter with fundamental accuracy," *IEEE Trans. Instrum. Meas.*, vol. 44, no. 2, pp. 223–225, Apr. 1995.

[24] S. P. Benz, A. Hamilton, C. J. Burroughs, T. E. Harvey, and L. A. Christian, "Stable 1-volt programmable voltage standard," *Appl. Phys. Lett.*, vol. 71, no. 13, pp. 1866–1868, Sep. 1997.

[25] C. J. Burroughs, P. D. Dresselhaus, Y. Chong, and H. Yamamori, "Flexible cryo-packages for Josephson devices," *IEEE Trans. Appl. Supercond.*, vol. 15, no. 2, pp. 465–468, Jun. 2005.

[26] *IEEE Standard for Digitizing Waveform Recorders*, IEEE Std. 1057-1994, (R2001).

[27] B. Jeanneret, F. Overney, A. Rüfenacht, and A. Mortara, "A high voltage Josephson-voltage-standard-locked synthesizer," in *Proc. CPEM*, Washington, DC, Jul. 1–6, 2012, pp. 670–671.

[28] A. Rüfenacht, C. J. Burroughs, S. P. Benz, and P. D. Dresselhaus, "A digital-to-analog converter with a voltage standard reference," in *Proc. CPEM*, Washington, DC, Jul. 1–6, 2012, pp. 436–437.

Alain Rüfenacht was born in La Chaux-de-Fonds, Switzerland, in 1975. He received the Ph.D. degree from the University of Neuchâtel, Neuchâtel, Switzerland, in 2005, for his work in collaboration with IBM Zurich Research Laboratory, on high-temperature superconducting ultrathin films.

In 1999, 2009, and 2010, he was a Scientific Collaborator with the Electrical Quantum Standards Laboratory, Federal Office of Metrology (METAS), Bern-Wabern, Switzerland. In 2007 and 2008 and since 2011, he is a Research Associate with the Quantum Voltage Project, National Institute of Standards and Technology, Boulder, CO, focusing mainly on the integration of Josephson junction arrays into voltage standards.

Charles J. Burroughs, Jr. was born on June 18, 1966. He received the B.S. degree in electrical engineering from the University of Colorado, Boulder, in 1988.

He is currently with the National Institute of Standards and Technology (NIST), Boulder, where he was first a student and has been a permanent staff member since 1988. At NIST, he has worked in the area of superconductive electronics, including the design, fabrication, and testing of Josephson voltage standards and digital-to-analog and analog-to-digital converters. He has 45 publications and is the holder of three patents in the field of superconducting electronics.

Mr. Burroughs was the recipient of three U.S. Department of Commerce Gold Medals for Distinguished Achievement.

Paul D. Dresselhaus was born in Arlington, MA, on January 5, 1963. He received the B.S. degree in physics and electrical engineering from the Massachusetts Institute of Technology, Cambridge, in 1985 and the Ph.D. degree in applied physics from Yale University, New Haven, CT, in 1991.

In 1999, he joined the Quantum Voltage Project at the National Institute of Standards and Technology, Boulder, CO, where he has developed novel superconducting circuits and broad-band bias electronics for precision voltage waveform synthesis and programmable voltage standard systems. He was with Northrop Grumman for three years, where he designed and tested numerous gigahertz-speed superconductive circuits, including code generators and analog-to-digital converters. He also upgraded the simulation and layout capabilities at Northrop Grumman to be among the world's best. He has also been a Postdoctoral Assistant with the State University of New York, Stony Brook, where he worked on the nanolithographic fabrication and study of Nb–AlOx–Nb junctions for single-electron and single flux quantum applications, single-electron transistors and arrays in Al–AlOx tunnel junctions, and the properties of ultrasmall Josephson junctions.

Dr. Dresselhaus was the recipient of two U.S. Department of Commerce Gold Medals for Distinguished Achievement and the 2006 IEEE Council on Superconductivity Van Duzer Prize.

Samuel P. Benz (M'01–SM'01–F'10) was born in Dubuque, IA, on December 4, 1962. He received the B.A. degree (*summa cum laude*) in physics and math from Luther College, Decorah, IA, in 1985 and the M.A. and Ph.D. degrees in physics from Harvard University, Cambridge, MA, in 1987 and 1990, respectively. He was awarded an R. J. McElroy Fellowship (1985–1988) to work toward the Ph.D. degree.

In 1990, he joined the National Institute of Standards and Technology (NIST), Boulder, CO, as a NIST/National Research Council Postdoctoral Fellow and became a permanent staff member in January 1992. He has been the Project Leader of the Quantum Voltage Project at NIST since October 1999. He has worked on a broad range of topics within the field of superconducting electronics, including Josephson junction array oscillators, single flux quantum logic, ac and dc Josephson voltage standards, Josephson waveform synthesis, and noise thermometry. He has over 160 publications and is the holder of three patents in the field of superconducting electronics.

Dr. Benz is a Fellow of the American Physical Society and a member of Phi Beta Kappa and Sigma Pi Sigma. He was the recipient of three U.S. Department of Commerce Gold Medals for Distinguished Achievement and the 2006 IEEE Council on Superconductivity Van Duzer Prize.